

TRANSIENT BEHAVIOR OF SEA URCHIN SPERM FLAGELLA FOLLOWING AN ABRUPT CHANGE IN BEAT FREQUENCY

BY DAN ESHEL¹, CHIKAKO SHINGYOJI², KENJIRO YOSHIMURA²,
BARBARA H. GIBBONS¹, IAN R. GIBBONS¹
AND KEIICHI TAKAHASHI²

¹*Pacific Biomedical Research Center, University of Hawaii, Honolulu, HI 96822, USA* and ²*Zoological Institute, Faculty of Science, University of Tokyo, Hongo, Tokyo 113, Japan*

Accepted 2 April 1990

Summary

Within the approximate range of 30–80 Hz, the flagellar beat frequency of a sea urchin sperm held by its head in the tip of a micropipet is governed by the vibration frequency of the micropipet. We have imposed abrupt changes in flagellar beat frequency by changing the vibration frequency of the micropipet within this range and used a high-speed video system to analyze the flagellar wave parameters during the first few cycles following the change. Our results demonstrate that the various flagellar beat parameters differ in the time they take to adjust to the new conditions. The initiation rate of new bends at the base is directly governed by the frequency of the vibration and changes immediately to the new frequency. The length and the propagation velocity of the developed bends become adjusted to the new conditions within approximately 1 beat cycle, whereas the bend angles take more than 4 beat cycles to attain their new steady-state value. Bends initiated shortly before the change in frequency occurs attain a final length and angle that depends on the relative durations of growth at the old and new frequencies. Our results suggest that the flagellar wavelength and bend angle are regulated by different mechanisms with the second not being directly dependent on bend initiation.

Introduction

A study of the transient response of an oscillating physical system to perturbations can provide information that cannot be obtained by observing and exploring the system at steady state. However, only a small number of studies on the parameters of flagellar beating have been performed under non-steady-state conditions (Gibbons, 1981, 1986; Rikmenspoel, 1978) compared to the number made on steady-state beating flagella (e.g. Goldstein, 1976; Eshel and Brokaw, 1987). To expand our limited knowledge of the mechanisms that control and regulate the direction, velocity and distribution along the axoneme of the sliding

Key words: flagella, bend parameters, transient behavior, control mechanism.

between doublet microtubules that is responsible for formation and propagation of bending waves, it is necessary to study the transient behavior of a flagellum in the few beat cycles following a sharp change in the conditions affecting the beating.

A recently introduced experimental technique makes it possible to study the behavior of a sperm flagellum under controlled mechanical conditions by holding its head at the tip of a vibrating micropipet that is being oscillated at the desired waveform, frequency and amplitude (Gibbons *et al.* 1987; Eshel and Gibbons, 1989). In these experiments, the flagellar beat frequency of the sperm is governed by the vibration frequency of the micropipet within the approximate range of 30–80 Hz (Gibbons *et al.* 1985). This procedure enables the introduction of mechanical events at timings that are synchronized with a specific phase of the beat cycle and, when used in combination with a high-speed video system, it permits an analysis of the transient behavior of sperm flagella during the beat cycles immediately after an abrupt change in parameters is induced.

In the present work, we analyze the waveform of a beating flagellum following an abrupt change in the vibration frequency of the micropipet in order to study the temporal and spatial effects that result from the induced change in flagellar beat frequency. Our results demonstrate that the various flagellar beat parameters differ in the time they take to adjust to the new conditions and suggest that mechanisms not directly dependent on bend initiation may control the different bending parameters.

Materials and methods

Sperm from the sea urchin *Hemicentrotus pulcherrimus* were diluted into Ca^{2+} -free artificial sea water containing 465 mmol l^{-1} NaCl, 10 mmol l^{-1} KCl, 25 mmol l^{-1} MgCl_2 , 28 mmol l^{-1} MgSO_4 , 5 mmol l^{-1} Tris-HCl and 0.2 mmol l^{-1} EDTA (pH 8.2). All experiments were done at room temperature.

We used an inverted microscope (Nikon Diaphot TMD) with phase-contrast optics ($\times 40$ objective magnification). The video system, which included the camera, the VHS cassette recorder and the stroboscopic illumination, was Nac model MHS 200 which records at a speed of $200 \text{ frames s}^{-1}$. The tip of the sperm head was held in the tip of a micropipet by gentle suction, and the micropipet was oscillated by a piezoelectric device (Corey and Hudspeth, 1980) which produces movement along the horizontal and/or vertical axis with a sensitivity of about $1.5 \mu\text{m V}^{-1}$. The device was mounted on the microscope stage on a model MO-103 Narishige hydraulic micromanipulator.

The voltage for driving the piezoelectric elements was synthesized by a real time computer program as described previously (Eshel and Gibbons, 1989). The micropipet was vibrated sinusoidally by applying sinusoidal voltage waveform to a bimorph on which the micropipet was attached. The design of software and hardware enables us to make abrupt changes in vibration frequency, and these were programmed to occur when the micropipet was at the leftmost position of its travel path on the monitor screen. The voltage waveform was continuously

recorded on the videotape, using a Nac high-speed video wave inserter (model V-96), so that the exact time at which the change in frequency occurred could be determined.

To obtain a clear effect, we chose to switch the vibration frequency between the lowest and highest frequencies at which the flagellum would beat normally with the bends propagating fully into the distal region of the flagellum (35–42 Hz and 58–65 Hz, respectively). The peak-to-peak amplitude of lateral vibration was 18 μm for all the experiments, and the sperm were vibrated approximately 20 μm above the glass slide. On every sperm that was caught, we performed 5–7 frequency changes from the low to the high frequency and back. The data from all the changes of a given sperm flagellum were superimposed with a time scale normalized to the time of the change in order to have a significant number of data points covering the whole range of the beat cycle.

Video images of sperm were traced, digitized and stored as values of angular orientation, and bending wave parameters were calculated as described previously (Eshel and Gibbons, 1989). The flagellar bends were numbered relative to time zero at which the change in frequency occurs (–1 for the last bend before the change in frequency occurs, and 1 for the first bend after the change, etc.) with a prefix of R for right and L for left bends, according to the direction of their convex sides on the monitor screen (Eshel and Gibbons, 1989).

Experiments were performed on seven sperm from different animals. The sperm flagella were about 45 μm long and their natural beat frequencies ranged between 47 and 50 Hz. Preliminary analysis showed that all sperm flagella responded in essentially the same manner to the change in frequency. The wave parameters of three sperm were analyzed in detail, and the data given below illustrate one typical example.

Results

Fig. 1A shows the movement of the tip of the micropipet during a frequency increase from 38 to 65 Hz and Fig. 1B shows corresponding movement during a decrease from 65 to 38 Hz. The data are composed of six (Fig. 1A) and five (Fig. 1B) instances of frequency change that are superimposed with respect to the time at which the change in voltage waveform, as shown by the video inserter, occurred (broken line).

The coincidence of the leftmost position of the micropipet with the time at which the change in the vibration frequency occurs in the voltage waveform demonstrates that the phase of the micropipet oscillations does not lag significantly behind that of the voltage that drives it. This, and the apparent instantaneous change in micropipet velocity when the frequency is changed, are indicators of the low Reynolds number characterizing the tip of the micropipet immersed in the solution. The smoothness of the plots that are derived from several superimposed instances of frequency change demonstrates that the movement of the micropipet before, during and after the change in frequency is reproducible.

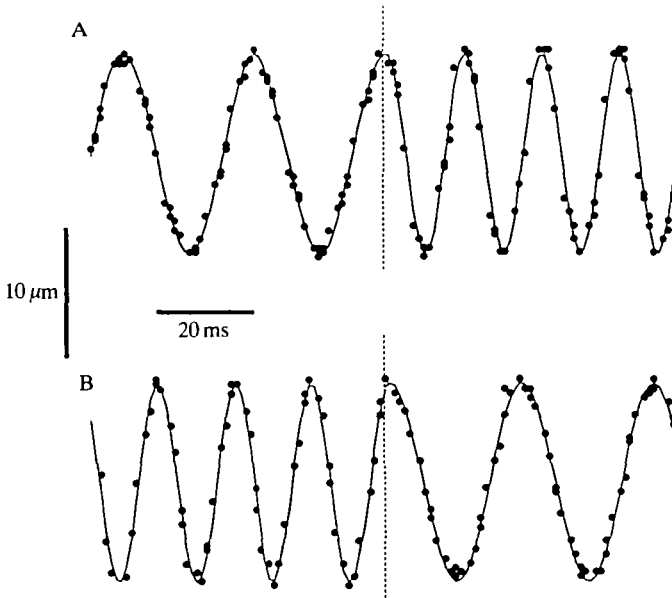


Fig. 1. Movement of the micropipet tip before, during and after a vibration frequency change (A) from 38 to 65 Hz and (B) from 65 to 38 Hz. The data are composed of six (A) and five (B) superimposed experiments (using the same sperm) with their times normalized to time zero at which the change in frequency occurred (broken line). The solid lines indicate sine waves that were fitted separately to the data before and after the change in frequency, using the Simplex method to vary the parameters for minimum root mean square deviation. The top of the figure corresponds to the left side and the bottom to the right side of the monitor screen.

The development of angle in newly formed bends is shown as a function of time in Fig. 2. Fig. 2A,B presents the angles of consecutive right and left bends (respectively) during a frequency increase, and Fig. 2C,D those during a frequency decrease. As can be seen, the initiation of bend R1 at the base of the flagellum is concurrent with the change in the vibration frequency in both cases within the range of the experimental error. Examination of the transient responses of the bend angles to the abrupt increase or decrease in beat frequency reveals that it takes approximately 3 beat cycles after this change before the angles of fresh, fully developed, bends attain the steady-state value characteristic of their new frequency. When the frequency increases from 38 to 65 Hz, the angle of fully developed bends falls from 2.6 to 2.0 rad for bends to either side (Fig. 2A,B), values similar to those obtained by C. Shingyoji, I. R. Gibbons, A. Murakami and K. Takahashi (in preparation). These values increase from 2.0 rad back to 2.6 rad when the frequency is changed back from 65 to 38 Hz (Fig. 2C,D). Note that the last left bend that is initiated just before the frequency increase (bend L-1) grows to practically the same maximal value as the previous left bends (Fig. 2B), whereas the L-1 bend initiated just before a frequency decrease appears to detect the change more rapidly, for it grows to a maximal angle of 2.2 rad, which is

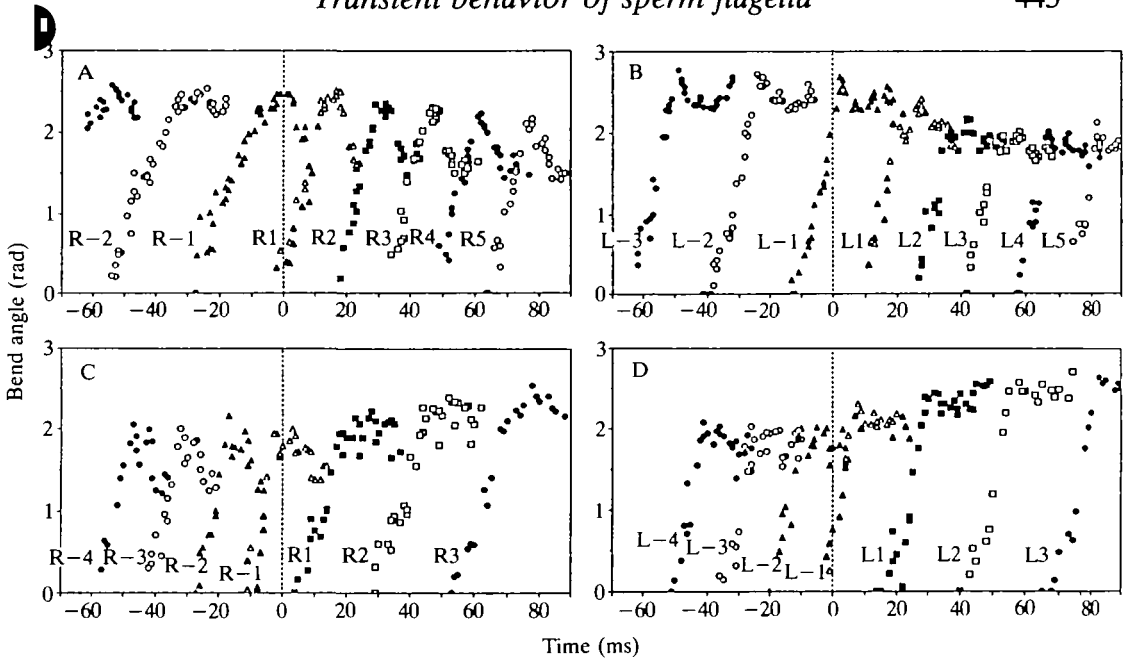


Fig. 2. Profiles of bend angle development as a function of time for experiments with frequency increase, (A) right bends, (B) left bends, and for experiments with frequency decrease, (C) right bends, (D) left bends. Data from six experiments are superimposed in A and B, and five in C and D. The beat frequency of the sperm before starting the vibration was 50 Hz. To clarify the presentation, data are shown for bends with their mid-position not more distal than $30\ \mu\text{m}$ from the base. Also, for clarity, different bends are presented with different symbols.

significantly greater than that of the previous left bends (Fig. 2D). The averages of bend angles from the three analyzed sperm which are presented in Table 1 show that the bend angles adjust to the new conditions within approximately 4 beat cycles.

Fig. 3 illustrates corresponding plots of the lengths of developing bends in order to demonstrate how the abrupt change in beat frequency affects the growth of bend length. It shows that the maximal lengths of successive fully developed bends adjust completely to the new frequency within only about 1 beat cycle. When the frequency is increased from 38 to 65 Hz, the maximal length of the fully developed right bends falls from 20 to $13\ \mu\text{m}$ (Fig. 3A) and that of the left bends from 18 to $12\ \mu\text{m}$ (Fig. 3B). These values increase back to 20 and $18\ \mu\text{m}$ when the frequency is changed back from 65 to 38 Hz (Fig. 3C,D). The other two sperm showed similar results. As described previously, bend growth occurs in two phases (Goldstein, 1976; Gibbons, 1981). The first phase starts when a bend is initiated at the base and ends when a new bend in the other direction is initiated. Then begins the second, faster phase that ends when the next bend in the same initial direction is initiated at the base of the flagellum. During steady-state beating, the differences in maximal bend lengths result mostly from changes in the relative durations of the

Table 1. Average angles and propagation velocities of bends before and after a change in vibration frequency

	Old frequency						New frequency						
Frequency increase													
Bend angle (rad)	2.55	2.55	2.57	2.53	2.55	2.53	2.50	2.33	2.20	2.13	2.10	2.08	2.08
Standard error	0.02	0.02	0.02	0.02	0.02	0.02	0.03	0.04	0.05	0.03	0.03	0.03	0.03
Velocity ($\mu\text{m ms}^{-1}$)	1.36	1.33	1.36	1.34	1.34	1.37	1.41	1.49	1.48	1.51	1.53	1.51	1.51
Standard error	0.01	0.02	0.01	0.02	0.02	0.02	0.02	0.02	0.01	0.03	0.02	0.02	0.02
Frequency decrease													
Bend angle (rad)	2.07	2.08	2.08	2.10	2.08	2.08	2.18	2.32	2.45	2.52	2.55	2.54	2.55
Standard error	0.03	0.03	0.03	0.04	0.03	0.03	0.03	0.04	0.06	0.03	0.02	0.02	0.02
Velocity ($\mu\text{m ms}^{-1}$)	1.49	1.48	1.55	1.53	1.53	1.53	1.35	1.32	1.33	1.33	1.32	1.29	1.33
Standard error	0.01	0.02	0.04	0.02	0.02	0.03	0.02	0.02	0.04	0.02	0.01	0.02	0.01

Data represent averages of left and right bends from three sperm. Bends are presented consecutively across the table from left to right. The data from left and right bends of all the sperm were averaged because *t*-tests at 95 % confidence limit showed no significant difference either between the mean angles of right and left bends of any given sperm or among the three sperm analyzed. Each individual value from which the averages of velocities were constructed is the slope of a single curve such as those in Fig. 4, starting when the trailing edge of the bend passes the point located $5 \mu\text{m}$ from the base along the flagellum. The slopes were calculated using linear least squares; the scatter of points for a typical bend corresponded to 7.7 % of the calculated slope at 90 % confidence limit.

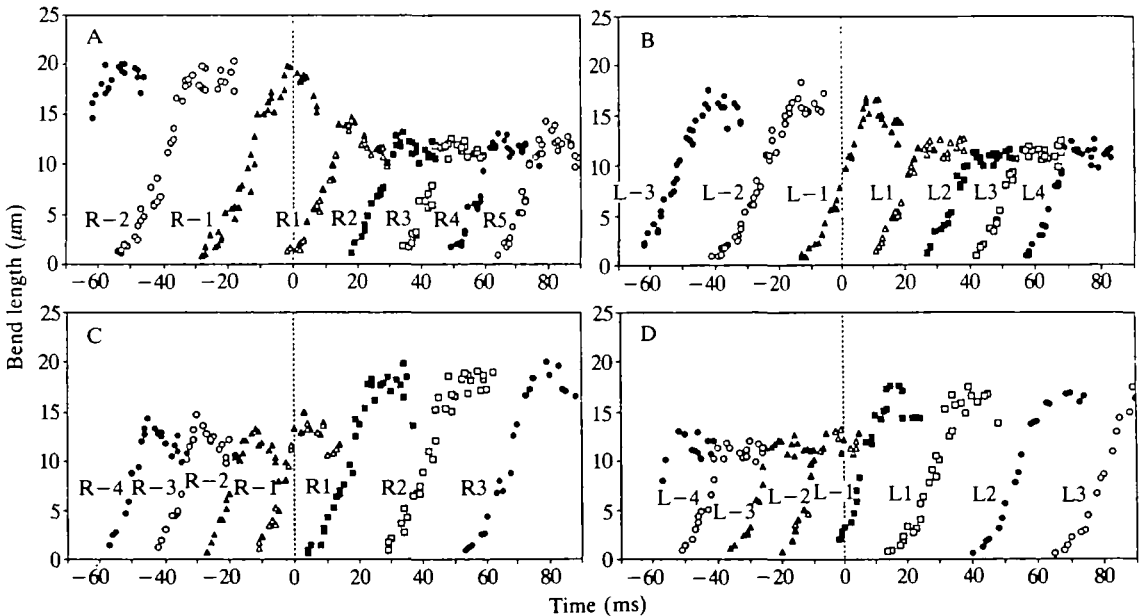


Fig. 3. Profiles of bend length development as a function of time. Details are the same as in the legend to Fig. 2.

growth during both phases. The distinctive growth pattern of the transitional bend L-1, which is initiated immediately before the change in frequency and continues to grow after the increase (Fig. 3B) or the decrease (Fig. 3D) of beat frequency has occurred, is even clearer here than with the bend angles. When the frequency increases, bend L-1 grows to practically the same length as the previous left bends (Fig. 3B), whereas when the frequency decreases, it grows to almost the same length as the following left bends (Fig. 3D).

When we extended the time for which images were analyzed up to 200 ms after the frequency change (not shown here), we noticed that there was a consistent slow upward drift (from 13 to 14.5 μm for the right bends and from 12 μm to 13 μm for the left bends) in the maximal length of fully developed bends of both sides that occurred subsequent to the initial decrease in length of the first bends initiated after the increase in frequency (R1, R2 in Fig. 3A and L1, L2 in Fig. 3B). It took approximately 6 beat cycles for the length of the fully developed bends to become stable at the steady-state value of the new frequency. This phenomenon was not observed after a decrease in beat frequency. This slow change possibly represents fine tuning of the bend parameters to the new hydrodynamic conditions, but, as it is a relatively small effect that we cannot fully explain, it will not be discussed further.

Fig. 4 shows the propagation velocity of right bends before, during and after the frequency is increased from 38 to 65 Hz. Data collected during a -frequency decrease showed essentially the same behavior. The average propagation velocities in regions distal to the first 5 μm from the three sperm are given in Table 1. The results show that the propagation velocities adjust to the new conditions within approximately 1 beat cycle. New data of greater precision would be necessary to determine the velocity of propagation within the proximal 5 μm of the flagellum.

To demonstrate the flow along the flagellum of information regarding the

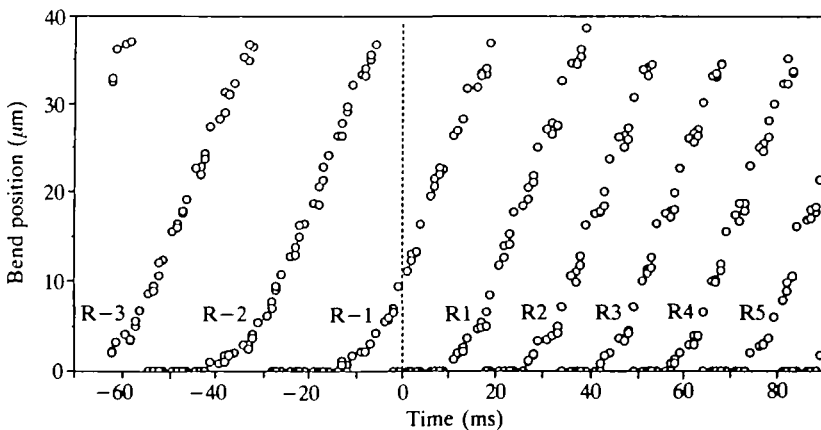


Fig. 4. A typical plot of position of the trailing edge of the bends as a function of time. The data presented here are for right bends in experiments of frequency increase.

change of frequency, we show in Fig. 5 the oscillation of shear angle (the angular orientation relative to the head center line) as a function of time at two different positions on the flagellum during an increase of vibration frequency, together with sine waves fitted separately to the data before and after the change in the frequency. At $3\ \mu\text{m}$ from the base (Fig. 5A), the oscillation starts to deviate from the old frequency 5.5–7.5 ms after the change occurs, whereas at $35\ \mu\text{m}$ from the base (Fig. 5B) it takes 24.0–27.5 ms before any change in the pattern of oscillation occurs. Assuming that information flows at a constant velocity along the flagellum, these data show that it flows at a velocity of $1.4\text{--}1.9\ \mu\text{m ms}^{-1}$. This is within the range of velocities at which fully developed bends propagate along the flagellum (Table 1). Similar data for the experiments on a decrease in vibration frequency (not shown) gave basically the same results.

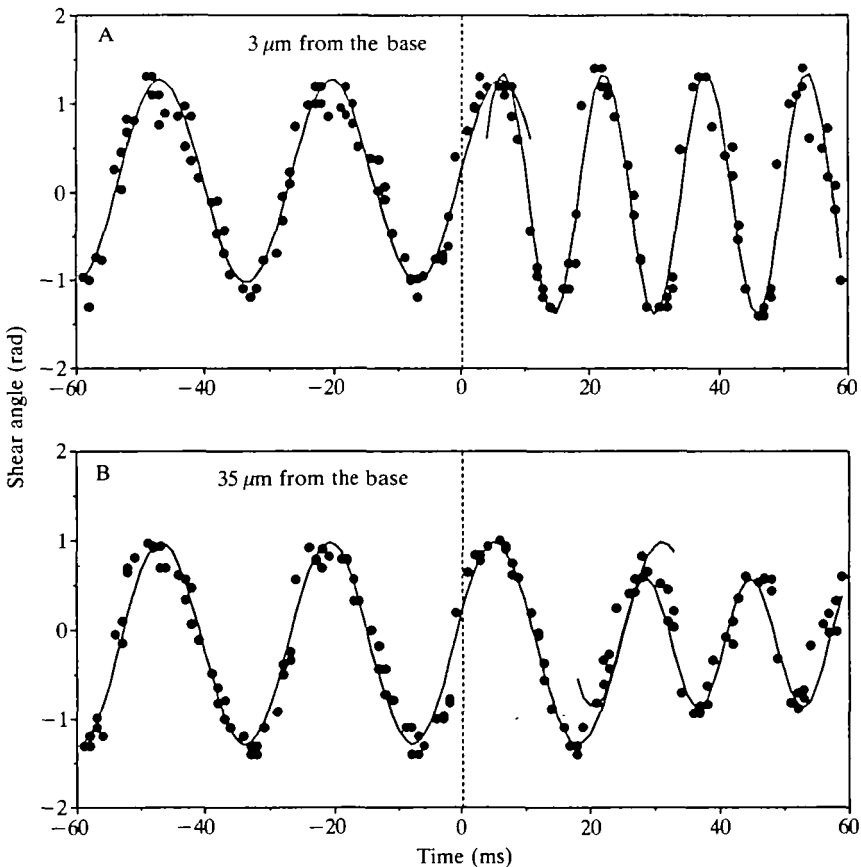


Fig. 5. The oscillations of shear angle with time at $3\ \mu\text{m}$ (A) and $35\ \mu\text{m}$ (B) from the base of the flagellum before and after a typical frequency increase. The solid lines indicate sine waves that were fitted separately to the data before and after the change in frequency, using the Simplex method to vary the parameters for minimum root mean square deviation.

Discussion

The present results demonstrate that the mechanism responsible for initiating new bends at the flagellar base is able to respond immediately to an abrupt change in the vibration frequency. However, the angles and lengths of fully developed bends show a delayed response to the change in the vibration frequency.

After reviewing the effects of different perturbing agents on flagellar beating parameters, Gibbons (1974) suggested that the mechanisms regulating beat frequency and flagellar waveform (mainly the bend angle) function separately, with only second-order interactions between them. Other more recent evidence supporting this hypothesis is the initial increase in beat frequency with no change in bend angle that occurs during digestion with trypsin (Brokaw and Simonick, 1977), the decrease in beat frequency with little change in bend angle after an increase in the concentration of LiCl in the reactivation solution (Brokaw, 1989) and the constant beat frequency associated with drastically altered waveforms that occur during the stopping transient that follows a sudden influx of Ca^{2+} (Gibbons and Gibbons, 1980).

The results presented in Figs 2 and 3 support and extend this hypothesis regarding the independence of waveform and beat frequency. A change in the vibration frequency of the micropipet is manifest immediately in the beat frequency of the flagellum; the length to which a fully developed bend grows, and the velocity with which it propagates, which are dictated primarily by the beat frequency, attain their new values within less than 1 beat cycle after the frequency is changed. However, the angle of the fully developed bends takes as much as 4 beat cycles to reach the new steady-state value. This difference in response time argues that the beat frequency and bend angle are regulated by two independent mechanisms.

Since the bend angle is related to the curvature of the bend, it is possible that the change in the bend angle following a change in beat frequency is composed of two components: an active component, the result of active sliding between doublet microtubules, and a passive component derived from elastic strains within the axoneme. It might be that the active component responds almost immediately to the change in the vibration frequency, as do the beat frequency and the length and propagation velocity of the developed bends, but the passive component lags in its response to the change, especially in regions far from the head. This explains the observed slower adjustment of the bend angle to the new conditions.

An alternative explanation is that ATP concentration is a limiting factor and that the local concentration remains sufficient to maintain large bend angles for a short time after a frequency increase, and that correspondingly the ATP concentration takes a certain time to be replenished after a decrease in beat frequency, since it has to diffuse along the flagellum from the mitochondria at the flagellar base. Similar experiments with imposed frequency changes on reactivated sperm flagella would determine the validity of this explanation.

It has been demonstrated previously that the capability for oscillation exists throughout the flagellum (Brokaw and Gibbons, 1973; Shingyoji *et al.* 1977). In

the present work (Fig. 5), we show that information regarding a change in oscillation frequency appears to travel along the flagellum at a velocity similar to that of bend propagation, and that two remote regions on the flagellum can oscillate for a time of around 1 beat cycle with different information about the oscillation frequency. This observation supports and extends the hypothesis that postulates autonomous oscillatory properties in short regions along the flagellum.

Little is known about the flagellar substructure that is responsible for regulating the oscillatory behavior of the flagellar machinery by coordinating the activity of the dynein arms along the axoneme. Several studies have suggested that the central-pair microtubules may coordinate sliding by rotating 360° synchronously with each beat cycle of the flagellum (Omoto and Kung, 1979; Omoto and Witman, 1981; Kamiya, 1982). It is possible that at the instant of frequency change a small twist in the central-pair microtubules is created at the base of the flagellum (due to the abrupt change in the rotation speed) and that this twist then propagates along the axoneme. During this time, regions distal to this twist will oscillate at the old frequency while regions proximal to it will oscillate at the new frequency. This model could account for the simultaneous oscillation at different frequencies at different positions along the flagellum illustrated in Fig. 5.

As was mentioned in the Results, the left bend that is initiated half a beat cycle before the change in frequency occurs (bend L-1 in Fig. 3) and whose second phase of growth continues after the change, reaches a length similar to that of the previous left bends when the frequency is increased, but grows to a length closer to that of the subsequent left bends when the frequency decreases. Since bends develop in pairs (Goldstein, 1976), the two developing basal bends are affected by changes occurring at the flagellar base, and the reason for the apparent hysteresis is probably that the relative duration of growth for bend L-1 at the new frequency is longer after a frequency increase (Fig. 3B) than after a frequency decrease (Fig. 3D). The fact that the pair of the basal bends developing at the time of the frequency change is affected by the change in the vibration frequency of the head suggests that the lateral movement of the micropipet and the head of the sperm affects directly the sliding occurring between the doublet microtubules in the first interbend region (Gibbons, 1981).

The general hypothesis that the parameters of fully developed bends are not affected by events that happen proximal to them was suggested by previous experimental results demonstrating normal propagation of pre-existing bends distal to a spot on the flagellum amputated by a laser microbeam (Goldstein, 1969) or blocked with a microneedle (Okuno and Hiramoto, 1976). Our observations support and extend this hypothesis by showing that the bend that has only partially developed and is starting to propagate is affected by the frequency change, whereas bends in more distal regions of the flagellum appear to be completely unaffected.

We thank Cheryl Phillipson for technical assistance. This work has been supported by grants from the National Institute of Health (USA) HD 06565 (to

BHG), grants-in aid for Scientific Research nos 61304007 and 62480016 from the Ministry of Education, Science and Culture of Japan (KT) and a grant from the Mitsubishi Foundation (KT). We would also like to thank the Japan Society for the Promotion of Science and the National Science Foundation (USA) (INT8716302) for funding our joint research through the USA–Japan Cooperative Science Program.

References

- BROKAW, C. J. (1989). Operation and regulation of the flagellar oscillator. In *Cell Movement*, vol. 1, *The Dynein ATPases* (ed. F. D. Warner, P. Satir and I. R. Gibbons), pp. 267–279. New York: Alan R. Liss, Inc.
- BROKAW, C. J. AND GIBBONS, I. R. (1973). Localized activation of bending in proximal, medial and distal regions of sea urchin sperm flagella. *J. Cell Sci.* **13**, 1–10.
- BROKAW, C. J. AND SIMONICK, T. F. (1977). Motility of Triton-demembrated sea urchin sperm flagella during digestion by trypsin. *J. Cell Biol.* **75**, 650–665.
- COREY, D. P. AND HUDSPETH, A. J. (1980). Mechanical stimulation and micromanipulation with piezoelectric bimorph elements. *J. Neurosci. Meth.* **3**, 183–202.
- ESHEL, D. AND BROKAW, C. J. (1987). New evidence for a “biased baseline” mechanism for calcium-regulated asymmetry of flagellar bending. *Cell Motil. Cytoskel.* **7**, 160–168.
- ESHEL, D. AND GIBBONS, I. R. (1989). External mechanical control of the timing of bend initiation in sea urchin sperm flagella. *Cell Motil. Cytoskel.* **14**, 416–423.
- GIBBONS, I. R. (1974). Mechanisms of flagellar motility. In *The Functional Anatomy of the Spermatozoon* (ed. B. A. Afzelius), pp. 127–140. New York: Pergamon Press.
- GIBBONS, I. R. (1981). Transient flagellar waveforms during intermittent swimming in sea urchin sperm. II. Analysis of tubule sliding. *J. Musc. Res. Cell Motil.* **2**, 83–130.
- GIBBONS, I. R. (1986). Transient flagellar waveforms in reactivated sea urchin sperm. *J. Musc. Res. Cell Motil.* **7**, 245–250.
- GIBBONS, I. R. AND GIBBONS, B. H. (1980). Transient flagellar waveforms during intermittent swimming in sea urchin sperm. I. Wave parameters. *J. Musc. Res. Cell Motil.* **1**, 31–59.
- GIBBONS, I. R., SHINGYOJI, C., MURAKAMI, A. AND TAKAHASHI, K. (1985). Effect of imposed head vibration on the beat of sea urchin sperm flagella. *J. Cell Biol.* **101**, 270a.
- GIBBONS, I. R., SHINGYOJI, C., MURAKAMI, A. AND TAKAHASHI, K. (1987). Spontaneous recovery after experimental manipulation of the plane of beat in sperm flagella. *Nature* **325**, 351–352.
- GOLDSTEIN, S. F. (1969). Irradiation of sperm tails by laser microbeam. *J. exp. Biol.* **51**, 431–441.
- GOLDSTEIN, S. F. (1976). Form of developing bends in reactivated sperm flagella. *J. exp. Biol.* **64**, 173–184.
- KAMIYA, R. (1982). Extrusion and rotation of the central-pair microtubules in detergent-treated *Chlamydomonas* flagella. *Cell Motil. Suppl.* **1**, 169–173.
- OKUNO, M. AND HIRAMOTO, Y. (1976). Mechanical stimulation of the starfish sperm flagella. *J. exp. Biol.* **65**, 401–413.
- OMOTO, C. K. AND KUNG, C. (1979). The pair of central tubules rotates during ciliary beat in *Paramecium*. *Nature* **279**, 532–534.
- OMOTO, C. K. AND WITMAN, G. B. (1981). Functionally significant central-pair rotation in a primitive eukaryotic flagellum. *Nature* **290**, 708–710.
- RIKMENSPÖEL, R. (1978). Movement of sea urchin sperm flagella. *J. Cell Biol.* **76**, 310–322.
- SHINGYOJI, C., MURAKAMI, A. AND TAKAHASHI, K. (1977). Local activation of Triton-extracted flagella by iontophoretic application of ATP. *Nature* **265**, 269–270.